Lasers in Manufacturing Conference 2021

Processing of low-alloyed case-hardening steel Bainidur AM by means of DED-LB/M

Dominic Bartels[a,b,*], Oliver Hentschel[a,b], Jonas Dauer[a], Wolfgang Burgmayr[a], Michael Schmidt[a,b]

[a] *Institute of Photonic Technologies, Friedrich-Alexander-Universität Erlangen-Nürnberg, Konrad-Zuse-Straße 3/5, 91052 Erlangen, Germany;*
[b] *Erlangen Graduate School in Advanced Optical Technologies (SAOT), Friedrich-Alexander-Universität Erlangen-Nürnberg, Paul-Gordan-Straße 6, 91052 Erlangen, Germany*

Abstract

Low-alloyed steels are typically exposed to additional case-hardening post-processing to improve the mechanical properties in the case area of the material for increased hardness and wear resistance. Another possibility for improving these material properties is provided by in-situ alloying using laser-based directed energy deposition of metals (DED-LB/M). However, this requires basic understanding of the mechanisms when processing the base material. Within this work, different processing parameters for defect-free fabrication of the low-alloyed case-hardening steel Bainidur AM are presented. This includes the correlation of geometrical properties and internal defects like pores or cracks with the applied process parameters. Additional hardness measurements are performed for analyzing the influence of different processing strategies. It is found that a hardness gradient is formed and that the material hardness is depending on the process parameters used. Furthermore, the obtained material hardness is similar to the hardness values of conventionally bainitized samples obtained from literature.

Keywords: Additive manufacturing; DED-LB/M; Laser metal deposition; Case-hardening steel; Bainidur AM

1. Introduction

Additive manufacturing technologies like powder bed fusion of metals using laser beam (PBF-LB/M) and direct energy deposition of metals using laser beam (DED-LB/M) are constantly gaining importance and relevance in industrial process chains [1]. Whereas the PBF-LB/M process is commonly used for the

* Corresponding author.
E-mail address: dominic.bartels@lpt.uni-erlangen.de .

manufacturing of geometrically highly complex products [2], DED-LB/M is mostly used for the repair or coating of parts [3]. However, over the last few years, the DED-LB/M technology has found an increasing interest in the field of additive manufacturing as near net-shape products with tailored material properties can be processed [4]. In DED-LB/M, the powder material is provided by a powder hopper and is transported into the process zone using a carrier gas stream and focused by a powder nozzle. A high-power laser is used for melting and bonding the metal to the substrate. By using several independent hoppers, different materials can be supplied into the processing zone, allowing for a flexible modification of the chemical composition of the specimen. The DED-LB/M process is characterized by high cooling rates compared to conventional manufacturing technologies like casting [5]. This favors the formation of a fine-grained and mostly dendritic microstructure, resulting in superior material properties compared to conventional products.

Up to now, several different types of materials like iron-, titanium-, or aluminum-based alloys have been successfully manufactured using the DED-LB/M technology [6]. In the field of high-alloyed steels, this includes stainless steels (e.g. 316L)[7] and tool steels (e.g. 1.2343)[8, 9], for which a wide range of parameters can be found for the successful and nearly defect-free processing of these alloys in literature. In contrast, low-alloyed steels like carburizing and nitrating steels (e.g. 16MnCr5 or 20MnCr5) have only barely been processed by means of DED-LB/M. However, investigations on the processing of these alloys using PBF-LB/M show that samples can be fabricated successfully from these materials using laser-based AM technologies [10, 11]. This group of material is interesting due to their wide range of industrial use in the fields of bearing technology and gear applications. Providing a fundamental knowledge on the manufacturing process, worn or defect parts made from case-hardening steels can be repaired or coated using DED-LB/M.

To tackle this information gap, fundamental investigations on the correlations between processing parameters and the geometrical properties of single weld tracks and single layer structures are studied within this work. Based on optical analysis, the weld track height and penetration depth as wells as the formed microstructure depending on the applied processing parameters are determined. Finally, the influence of different process parameters on the material hardness of the additively manufactured samples is determined for single- and multi-layer structures.

2. Materials and Methods

All experiments are performed on an ERLASER UNIVERSAL 50349 machine (ERLAS GmbH, Erlangen, Germany) with an integrated five-axis DED-LB/M cell. The laser-processing cell is equipped with a Laserline LDF 4000-4 4 kW diode laser with a characteristic wavelength of 900 - 1,080 nm (Laserline GmbH, Mülheim-Kärlich, Germany). Based on an adjustable telescope lens system, the laser spot size can be varied from 1 mm to 3.4 mm. The laser cell is equipped with two independent powder hoppers for supplying the powder material. Argon of type 4.6 is used for both shielding and carrier gas.

As powder material, the recently developed case-hardening steel Bainidur AM (Deutsche Edelstahlwerke Specialty Steel GmbH & Co. KG, Witten, Germany) is used. The powder morphology of the gas-atomized powder material is provided in Fig. 1.

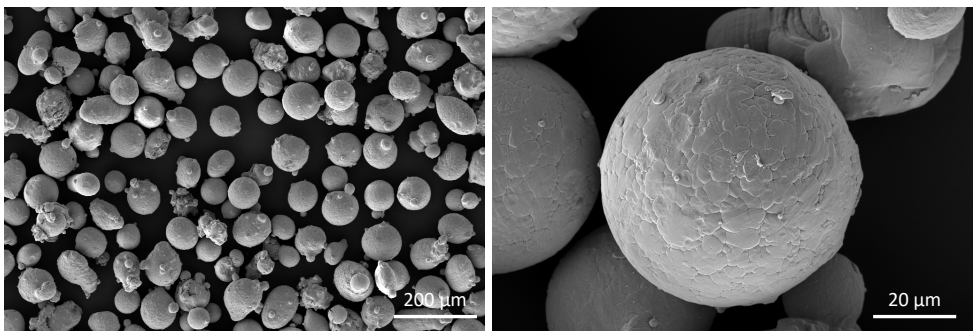

Fig. 1. (a) Powder particle morphology and (b) particle size distribution of Bainidur AM

Analysis of the particle size distribution shows d_{10}, d_{50}, and d_{90} values of 58.8, 80.8, and 100.4 µm, respectively. The powder consists of mainly spherical particles and some aspheric, peanut-shaped particles, which is suitable for the DED-LB/M process. In the first step, single weld tracks are manufactured with different laser powers, feed rates, laser spot diameters, and powder mass flows. The powder mass flow is determined experimentally by weighing the transported powder after a defined time of two minutes. Based on the obtained results for three independent measurements, the mass flow is determined in g/min. Shielding gas flow and carrier gas flow are set constant to 20 L/min and 4 L/min, respectively. Overlap between two weld tracks is maintained at 50 % of their single weld track width. Table 1 shows the investigated process parameter window. The samples are fabricated onto circular blanks (diameter 60 mm, thickness 3.5 mm) made from 16MnCr5 (1.7131) steel.

Table 1. Process parameters for DED-LB/M experiments

Process parameter	Values
Laser power [W]	400, 500, 600, 700, 800
Feed rate [mm/min]	400, 600, 800
Powder mass flow [g/min]	2.55, 4.11, 5.79
Spot size [mm]	1.5, 2.4
Number of layers [n]	1, 4
Shielding gas [L/min]	20
Carrier gas [L/min]	4
Overlap [%]	50

All manufactured specimens are embedded in a cold embedding resin, polished to 1 µm, and etched using a 3-% Nital solution. Next, images of these cross-sections are made using an optical light microscopy from Zeiss. For weld tracks, the width and height as well as the welding penetration depth are determined. The information on the width of the weld tracks is then used for manufacturing multilayer quadratic specimens with an edge-length of 15 mm in x-y-direction. First, the inner hatching of the structure is fabricated by positioning several overlapping weld tracks next to each other. The offset between two tracks is set to 50 % of the weld track width. This leads to a varying number of weld tracks for the different process parameters when manufacturing the specimens. In the next step, the hatching is followed by four contour track. For multilayer samples, the building pattern is rotated by 90 °, thus changing the starting point for consecutive layers.

Again, the manufactured samples are prepared metallographically according to the previously mentioned approach. Furthermore, Vickers hardness is determined on polished cross-sections using a microhardness indenter of type HP30S (Hegewald & Peschke Meß- und Prüftechnik GmbH, Nossen, Germany). Hardness measurements are performed based on a multi-column grid. The grid has a defined offset between the measurement points in y- and z-direction. An exemplary sketch of the building pattern for DED-LB/M samples and the hardness measurement grid is provided in Fig. 2.

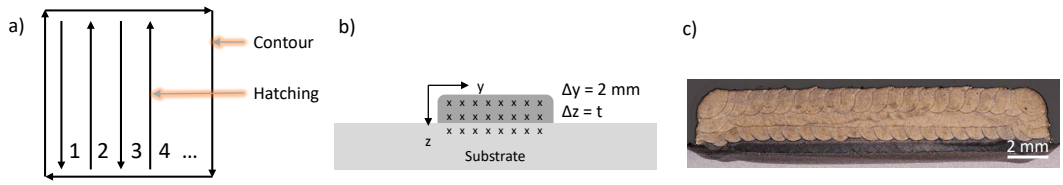

Fig. 2. (a) Scan pattern and (b) hardness measurement grid (c) and four-layer DED-LB/M manufactured samples (600 W, 400 mm/min)

The distance between two measurement points in y-direction is set constant to 2 mm. By this, the hardness inside one layer is represented. In z-direction, the offset between two measurement points is selected to be the height of the layer t. Both the lowest and highest determined hardness values of each layer are excluded from the analysis.

3. Results and Discussion

First, single weld tracks are manufactured for the presented parameter combinations. Microscopic analysis of cross-sections of these weld tracks shows that the geometrical properties like track width and track height are highly dependent on the applied processing strategy. An overview of these correlations for the powder mass flow of 2.55 g/min and two different spot sizes (d_L = 1.5 mm and 2.4 mm) is shown Fig. 3.

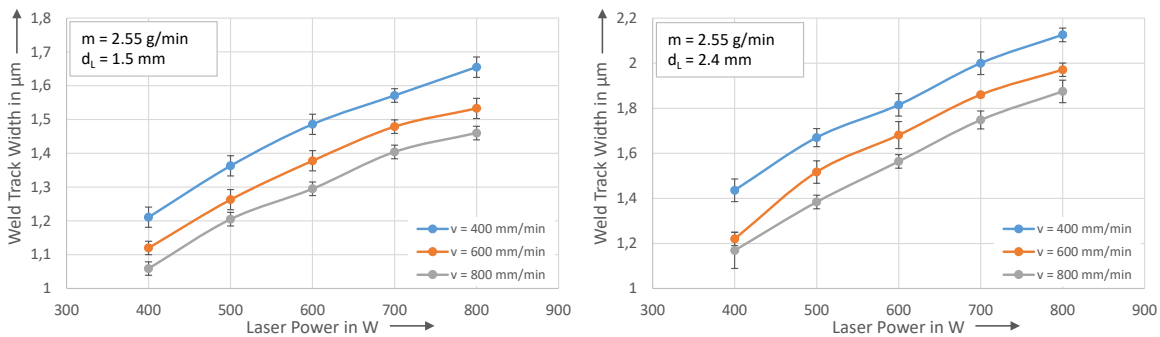

Fig. 3. Correlation between laser power and weld track width for different spot sizes of (a) 1.5 mm and (b) 2.4 mm

The width of the weld track is highly dependent on both laser power and laser spot size. Here, a linear increase can be observed for an increased laser power within the investigated parameter range. This effect can be attributed to the increased size of the melt pool for higher laser powers. Furthermore, the size of the melt pool is also affected by the selected spot size. The width of the weld track again increases linearly for higher laser powers. In contrast to this, higher feed rates lead to a reduced weld track width. This can be attributed to the main effect that the size of the melt pool is lowered to the reduced line energy input for high

feed rates compared to low feed rates. Therefore, to meet the reduced weld track width, a higher laser power is recommended.

In the next step, the influence of the powder mass flow on the weld track geometry is investigated. Therefore, the weld track and height for three different powder mass flow rates is compared in Fig. 4.

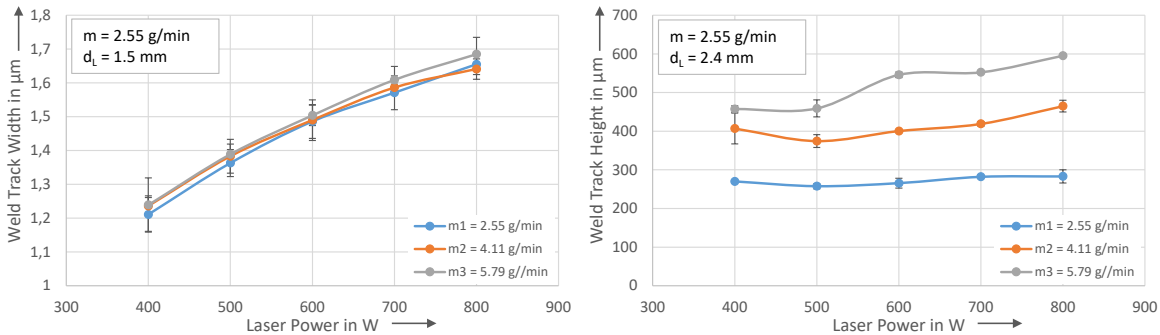

Fig. 4. Dependencies between (a) laser power and weld track width (b) laser power and weld track height

For comparison, the feed rate and laser spot size are kept constant at 400 mm/min and 1.5 mm, respectively. The investigation show that the width of the weld track is only barely depending on the powder mass flow. However, larger mass flows result in a higher build up rate of the weld tracks. Irregularities can be found for low laser powers in the range of 400 W when increasing the powder mass flow. These discrepancies are attributed to the fact that the supplied energy leads to an insufficient melting of the caught powder. For the powder mass flow m_3, this can be observed throughout the entire height of the weld track. Here, a higher laser power is recommended to melt the supplied powder material.

Multi-layer specimens

Based on the obtained results, one-layer structures are manufactured for the three powder mass flows. An exemplary overview of one-layer specimen is presented in Fig. 5.

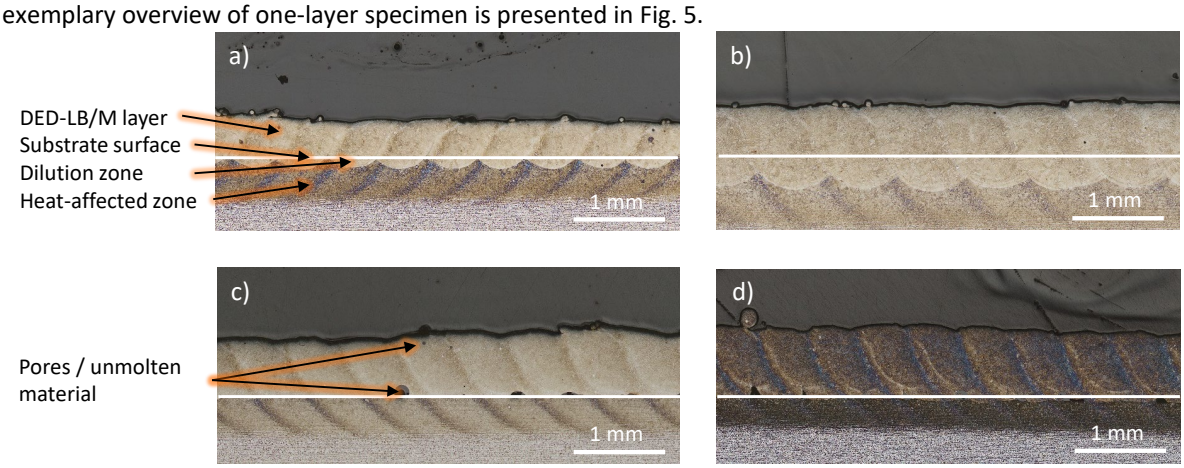

Fig. 5. Dilution and heat-affected zone of one-layer specimens manufactured with different laser powers and powder mass flows (a) 400 W, 2.55 g/min, (b) 600 W, 2.55 g/min, (c) 400 W, 4.46 g/min, and (d) 400 W, 6.32 g/min

From these images, it can be seen that a laser power of 400 W is too low for manufacturing structures additively as pores and non-molten powder can be found in the bonding area (Fig a), c), d)). Density analyses show a relative part density of > 99.7 % in the additively manufactured structure for a laser power above 600 W. Below that, lower part densities are observed due to unmolten powder and defects in the bonding zone. Furthermore, due to the non-existent dilution zone, the occurring defect will propagate along build direction and lead to delamination of the layers. In contrast, specimens manufactured with a higher laser power (Fig. b)) possess a larger dilution zone, showing that laser powers below 600 W are barely feasible for manufacturing Bainidur AM samples by means of DED-LB/M. From these structures, the layer height is determined experimentally using optical light microscopy. The average layer height for different feed rates and powder mass flows is presented in Table 2.

Table 2: Experimentally determined layer heights in µm for one-layered specimens for feed rates of 400 mm/min and 600 mm/min

	m_1 = 2.55 g/min	m_2 = 4.11 g/min	m_3 = 5.79 g/min
v = 400 mm/min	450 µm	650 µm	700 µm
v = 600 mm/min	350 µm	450 µm	550 µm

It was found that the layer height is not or only barely affected by the spot size and the laser power. In contrast, feed rate and powder mass flow significantly affect the height of the layer. With different sizes of these structures, changes in material properties can be assumed, as the size of the melt pool and the corresponding cooling conditions change for different parameter sets. Therefore, multilayer specimens are manufactured for a laser power of 600 W, two feed rates of 400 and 600 mm/min, and a constant powder mass flow of 2.55 g/min. Fig. 6 provides optical images on etched cross-sections.

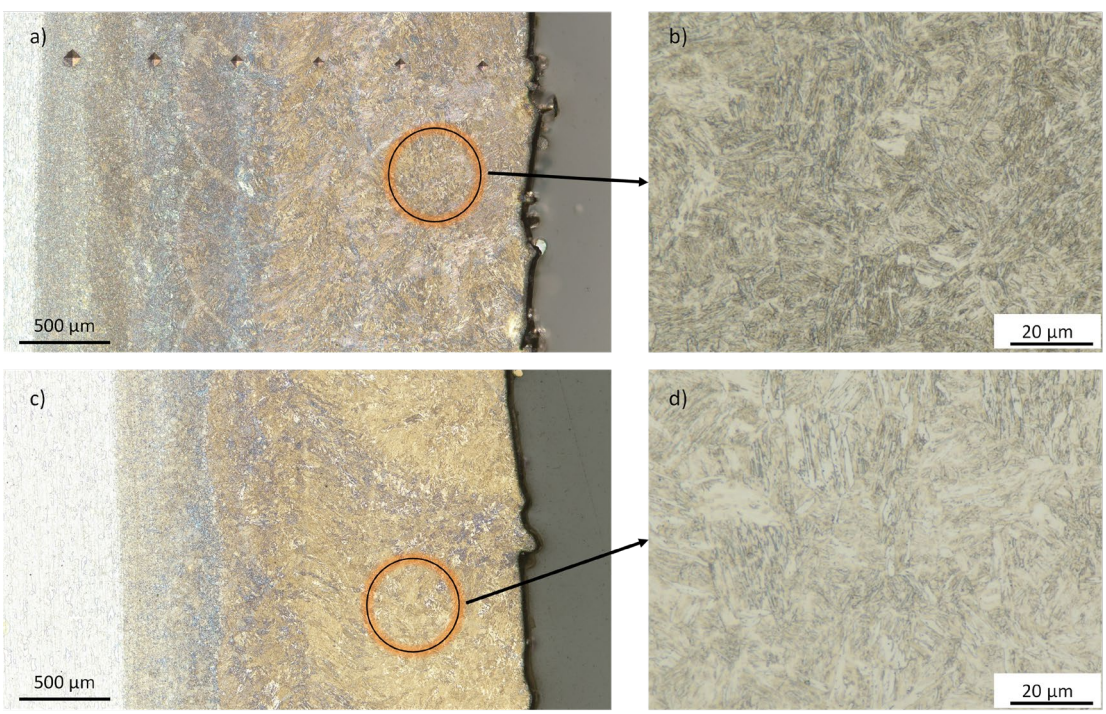

Fig. 6. Microstructure formation along build direction for a) and b) 600 W, 400 mm/min and c) and d) 600 W, 600 mm/min

From the optical images a relative density above 99.7 % is observed for the additively manufactured structure, independent of the applied process parameters. Furthermore, differences in the microstructure can be identified for the different process parameters, as the strength of the etching is pronounced differently. In both cases, a mixed structure consisting of shapes similar to the pearlite grain and martensitic or bainitic phase are found. The formation of the martensitic or bainitic phase is favored by the high cooling rates of the DED-LB/M process. When manufacturing multilayer specimens, the continuous reheating of the lower layers might surpass the bainite starting temperature, therefore supporting the formation of an ultra-fine bainitic phase. However, for fully proving this effect, additional investigation on the phase formation and the material hardness is necessary.

Analysis of material hardness

In a final step, the hardness of the additively manufactured specimens is determined for different processing strategies using the indentation tester. For one-layer samples, the material hardness is plotted from top surface towards substrate in Fig. 7. Different parameter combinations between 600 W and 800 W as well as 400 mm/min and 600 mm/min were used for fabricating these specimens.

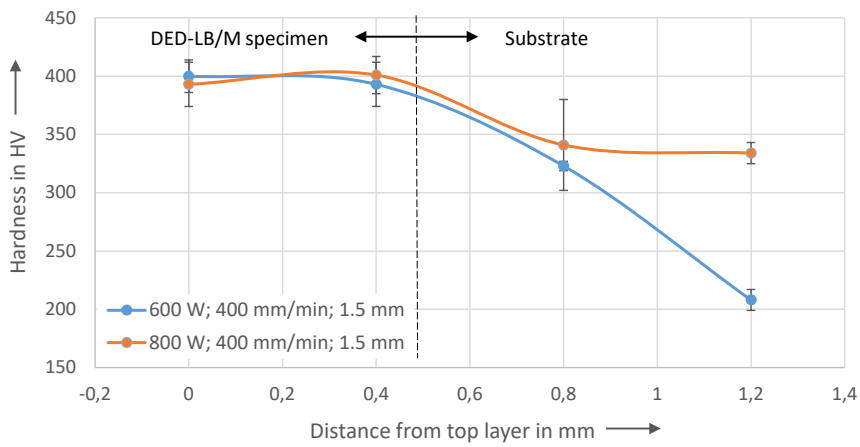

Fig. 7. Hardness gradient for DED-LB/M samples manufactured with different process parameter combinations

Analyses of the hardness of the additively manufactured sample shows no obvious difference in material hardness for the different laser powers. However, when increasing the laser power, an increased hardness can be determined within the substrate. This is attributed to both mixing effects in the bonding zone due to a higher weld penetration depth and an energy-induced hardening. The increased carbon content of the Bainidur AM powder compared to the 16MnCr5 favors the hardening effects of the base material. When moving further into the substrate, a similar hardness is observed for both samples manufactured with the presented parameter set. Furthermore, changes in the material hardness can be observed for two different laser spot diameters. This effect is presented in Fig. 8.

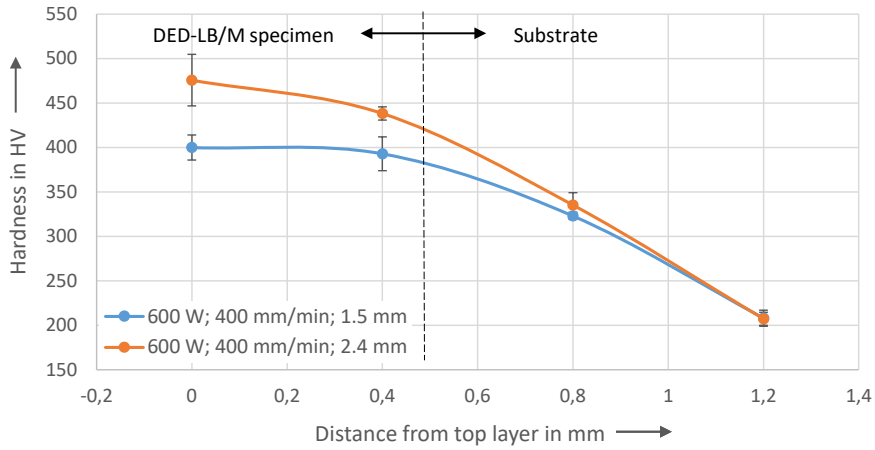

Fig. 8. Material hardness gradient for two different spot sizes (1.5 and 2.4 mm) and a constant laser power and powder mass flow

When increasing the laser spot, the width of the melt pool is increased. However, when maintaining the laser power constant, the weld penetration depth is lowered for larger spot sizes due to a reduced intensity. This leads to a larger surface area of the melt pool, resulting in a faster cooling of the liquid material. Thus, a fine-grain formation is supported, leading to the observable increase in material hardness for the top layers. When scaling the process towards four-layer structures, the effect can also be observed along build direction. An exemplary hardness gradient for two different process parameter sets is presented in Fig. 9.

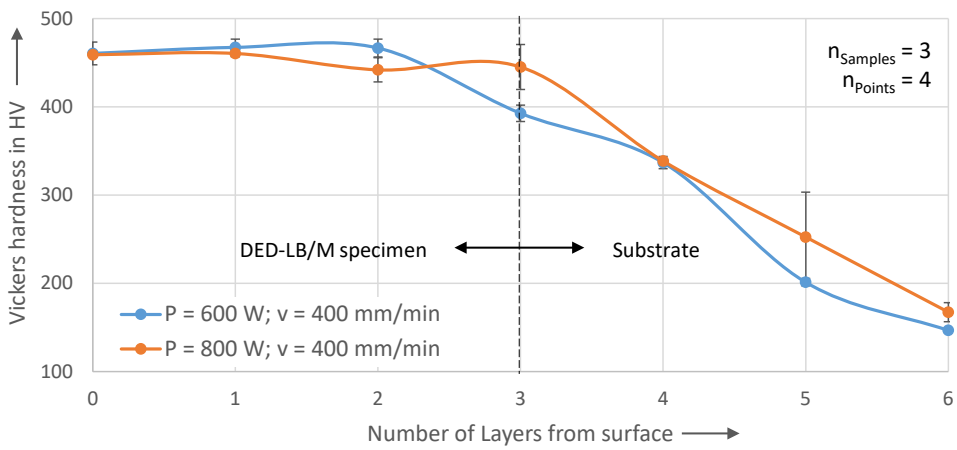

Fig. 9. Material hardness for four-layer specimens from top surface to substrate for a constant spot size (1,5 mm) and powder mass flow (2.55 g/min)

For four-layered specimens, the maximum hardness in the top layer is increased compared to one-layer samples. This can be explained by the lower carbon content of the substrate material (16MnCr5). The difference in carbon is approximately 0.1 wt.-%, thus significantly reducing the achievable material hardness. When processing multi-layer specimens, no significant changes in material hardness are observed for the top

three layers. Here, a homogeneous hardness is determined. This can be attributed to the fast cooling of these layers, supporting the formation of a bainitic/martensitic phase. However, for lower layers close to the dilution zone, an increase in material hardness is detected for the higher laser power. One possible explanation for this effect is the increased weld penetration depth for a laser power of 800 W. When studying the isothermal transformation diagram of the similar bainitic alloy Bainidur 7980 CN (Deutsche Edelstahlwerke Specialty Steel GmbH & Co. KG, Witten, Germany), a very low holding time around one minute can be identified for the formation of the bainitic phase [12]. Thus, the increased laser power could potentially favor the formation of this phase, which can also be assumed from the hardness values of around 430 HV. However, for fully assessing these effects, further investigations on the microstructure formation along build direction are necessary, which will be performed in future work.

4. Conclusion

The present work shows results on the processing of Bainidur AM by means of DED-LB/M. Preceding investigations on the correlations between process parameters and weld track geometry are presented, laying the foundation for the generation of layer-by-layer structures. It was found that a defect-free manufacturing of samples is possible for different process parameter combinations for laser powers between 600 W and 800 W. Laser powers below 600 W result in an insufficient melting of the powder material, leading to defects in the bonding zone.

Furthermore, the material hardness was determined for different process parameter combinations. It was found that the hardness increases for larger spot sizes, which can be attributed to a faster cooling. For multi-layered specimens, a higher material hardness is observed for higher laser powers in lower-lying layers. A possible reason for this is the phase transformation behavior of the at least partially bainitic microstructure. Due to the repetitive energy input into these layers, the bainite start temperature and the corresponding cooling times necessary for forming the bainitic phase might be surpassed. Future work will focus on the investigation of the microstructure formation along build direction for fully assessing the observed effect.

Acknowledgements

The authors would like to thank the Bundesministerium für Wirtschaft und Energie (BMWi) for funding the project "Ressourcenminimale Fertigung durch hybride und hochvernetzte Prozesse“.

The authors gratefully acknowledge funding of the Erlangen Graduate School in Advanced Optical Technologies (SAOT) by the Bavarian State Ministry for Science and Art.

In addition, the authors would like to thank the Deutsche Edelstahlwerke Specialty Steel GmbH & Co. KG, Witten, Germany, for providing the powder material for performing the DED-LB/M experiments.

References

[1] *Gasser, A.; Backes, G.; Kelbassa, I. et al.:* Laser Additive Manufacturing. *In:* Laser Technik Journal 7 (2010), Heft 2, S. 58-63. https://doi.org/10.1002/latj.201090029.

[2] *Schmidt, M.; Merklein, M.; Bourell, D. et al.:* Laser based additive manufacturing in industry and academia. *In:* CIRP Annals 66 (2017), Heft 2, S. 561-583. https://doi.org/10.1016/j.cirp.2017.05.011.

[3] *Graf, B.; Gumenyuk, A.; Rethmeier, M.:* Laser Metal Deposition as Repair Technology for Stainless Steel and Titanium Alloys. *In:* Physics Procedia 39 (2012), S. 376-381. https://doi.org/10.1016/j.phpro.2012.10.051.

[4] *Thivillon, L.; Bertrand, P.; Laget, B. et al.:* Potential of direct metal deposition technology for manufacturing thick functionally graded coatings and parts for reactors components. *In:* Journal of Nuclear Materials 385 (2009), Heft 2, S. 236-241. https://doi.org/10.1016/j.jnucmat.2008.11.023.

[5] *Amine, T.; Newkirk, J.W.; Liou, F.:* An investigation of the effect of direct metal deposition parameters on the characteristics of the deposited layers. *In:* Case Studies in Thermal Engineering 3 (2014), Heft 2, S. 21-34. https://doi.org/10.1016/j.csite.2014.02.002.

[6] *Mahamood, R.M.:* Laser Metal Deposition Process of Metals, Alloys, and Composite Materials. Springer International Publishing, Cham, 2018.

[7] *Sun, G.F.; Shen, X.T.; Wang, Z.D. et al.:* Laser metal deposition as repair technology for 316L stainless steel: Influence of feeding powder compositions on microstructure and mechanical properties. *In:* Optics & Laser Technology 109 (2019), S. 71-83. https://doi.org/10.1016/j.optlastec.2018.07.051.

[8] *Rabiey, M.; Schiesser, P.; Maerchy, P.:* Direct Metal Deposition (DMD) for Tooling Repair of DIN 1.2343 Steel. *In:* Procedia CIRP 95 (2020), Heft 10, S. 23-28. https://doi.org/10.1016/j.procir.2020.01.151.

[9] *Hentschel, O.; Siegel, L.; Scheitler, C. et al.:* Processing of AISI H11 Tool Steel Powder Modified with Carbon Black Nanoparticles for the Additive Manufacturing of Forging Tools with Tailored Mechanical Properties by Means of Laser Metal Deposition (LMD). *In:* Metals 8 (2018), Heft 9, S. 659. https://doi.org/10.3390/met8090659.

[10] *Bartels, D.; Klaffki, J.; Pitz, I. et al.:* Investigation on the Case-Hardening Behavior of Additively Manufactured 16MnCr5. *In:* Metals 10 (2020), Heft 4, S. 536. https://doi.org/10.3390/met10040536.

[11] *Schmitt, M.; Kamps, T.; Siglmüller, F. et al.:* Laser-based powder bed fusion of 16MnCr5 and resulting material properties. *In:* Additive Manufacturing 35 (2020), Heft 73, S. 101372. https://doi.org/10.1016/j.addma.2020.101372.

[12] *Deutsche Edelstahlwerke Specialty Steel GmbH & Co. KG:* Bainidur 7980 CN – Bainitischer Stahl für die Serienproduktion.